Distribution Agreement

In presenting this thesis as a partial fulfillment of the requirements for a degree from Emory University, I hereby grant to Emory University and its agents the non-exclusive license to archive, make accessible, and display my thesis in whole or in part in all forms of media, now or hereafter now, including display on the World Wide Web. I understand that I may select some access restrictions as part of the online submission of this thesis. I retain all ownership rights to the copyright of the thesis. I also retain the right to use in future works (such as articles or books) all or part of this thesis.

Signature:

J.K.D.T.
Janielle K. Taylor

04/17/2013
Date

The use of micro-magnetic resonance imaging (micro-MRI) to study morphological changes in the cochlea of conditional connexin26 (cCx26) null mice

by

Janielle K. Taylor

Xi (Erick) Lin, Ph.D.
Adviser

Neuroscience and Behavioral Biology Program

Xi (Erick) Lin, Ph.D.
Adviser

N. Wendell Todd, MD, MPH
Committee Member

Paul R. Lennard, Ph.D.
Committee Member

Wendy L. Newby, Ph.D.
Committee Member

April 17, 2013
Date

The use of micro-magnetic resonance imaging (micro-MRI) to study morphological changes in the cochlea of conditional connexin26 (cCx26) null mice

By

Janielle K. Taylor

Xi (Erick) Lin, Ph.D.
Adviser

An abstract of
A thesis submitted to the Faculty of Emory College of Arts and Sciences
of Emory University in partial fulfillment
of the requirements of the degree of
Bachelor of Sciences with Honors

Neuroscience and Behavioral Biology Program

2013

Abstract

The use of micro-magnetic resonance imaging (micro-MRI) to study morphological changes in the cochlea of conditional connexin26 (cCx26) null mice
By: Janielle K. Taylor

Sensorineural hearing loss (SNHL) is the most common type of hearing loss worldwide, effecting one in every 500 newborns. Yet, the underlying cause is typically unknown. One important reason is that the inner ear cannot be biopsied directly without compromising hearing. Furthermore, intracochlear cells have not been imaged with resolution sufficient to establish diagnosis. Imaging cells within the cochlea is technologically difficult because of the cochlea's small size and encasement in bone (the cochlear shell is among the densest bones in the body). Magnetic resonance imaging (MRI) enables non-invasive imaging of tissues in biological specimens ranging from mice to human beings. There is growing interest in performing high-resolution MRI studies at the scale of resolving individual cells. Few studies have reported successful visualization of the structures of the inner ear. None have investigated morphological changes in mouse models of genetic deafness. In this work, we aimed to compare high-resolution MRI examinations of inner ear structures at 9.4T with high-power evaluation of osmium- stained plastic-embedded, serial sections through the inner ear. Our results suggest that the MRI results we currently obtained have sufficient resolution to resolve major landmarks of the cochlear and vestibular structures (e.g., scala media, scala tympani, spiral osseous laminar, etc). However, the protocol we used so far was not sufficient to resolve individual cochlear cells for a diagnosis at the cellular level for the cCx26

null mouse model. I will discuss possible improvements and future development of optical tools and techniques (such as those based on two-photon micro-endoscopy) to better study morphological changes associated with SNHL.

Abbreviations

A = Apical Turn
ABR = Auditory brainstem response
AC = Anterior Canal
ARNSHL = Autosomal recessive non-syndromic hearing loss
B = Basal Turn
CA = Cochlear aqueduct
CC = Claudius Cell
C = Cochlea
CT = computed tomography
CX26 = Homo sapien connexin 26 (GJB2 product)
Cx26 = Mus musculus connexin 26 (Gjb2 product)
CX30 = Homo sapien connexin 30 (GJB6 product)
Cx30 = Mus musculus connexin 30 (Gjb6 product)
dB = Decibel
DC = Deiter Cell
DFNA3 = Autosomal dominant non-syndromic hearing loss locus (GJB2/GJB6)
DFNB1 = Autosomal recessive non-syndromic hearing loss locus (GJB2/GJB6)
ED = Endolymphatic duct
ES = Endolymphatic sac
H = Helicotrema
Hc = Hensen Cell
HC = Horizontal Canal
IHC = Inner hair cell
IST = Inner Spiral Tunnel
M = Modiolus

OC = Organ of Corti

OHC = Outer hair cell

OSL = Osseous Spiral Lamina

Mod = Modiolus

M = Middle Turn

NSHL = Non-syndromic Hearing Loss

Pc = Pillar Cell

PC = Posterior Canal

R = Round Window

RM = Reissner's Membrane

S = Saccule

SGN = Spiral ganglion neuron

SM = Scala Media

SNHL = Sensorineural hearing loss

St = Stapes

ST = Scala Tympani

SV = Scala Vascularis

TC = Tunnel of Corti

TM = Tectorial Membrane

U = Utricle

C = Cochlea

The use of micro-magnetic resonance imaging (micro-MRI) to study morphological changes in the cochlea of conditional connexin26 (cCx26) null mice

By

Janielle K. Taylor

Xi (Erick) Lin, Ph.D.
Adviser

A thesis submitted to the Faculty of Emory College of Arts and Sciences
of Emory University in partial fulfillment
of the requirements of the degree of
Bachelor of Sciences with Honors

Program in Neuroscience and Behavioral Biology

2013

Acknowledgements

In 1961, Dr. Georg von Békésy accepted the Nobel Prize in Physiology or Medicine for his work in describing how sound waves are discriminated in the inner ear. During his Nobel Lecture, Dr. von Békésy said, "I must admit that I have never liked to work hard. Preparing for college examinations was something I could do, but I hated to do it. Even today, I dislike deadlines. But there is one thing I am always ready to do, and that is to look at beautiful things." The ear is one of those beautiful things, and I would like to thank Dr. von Békésy for opening doors for me to study it's amazing form and function.

I would never have been able to finish my honors thesis without the guidance of my committee members, help from friends, and support from my family.

I would like to express my deepest gratitude to my advisor, Dr. Erick Lin, for his excellent guidance, patience, and providing me with an excellent atmosphere for doing research. I would also like to thank Dr. Qing Chang, for his assistance in this project. Dr. Qing Chang prepared the samples for MRI, and was instrumental in helping me analyze the data collected. Many thanks to Dr. Grant Kim and other researchers in the laboratory of Dr. Lin for helping me collect samples and prepare this manuscript. Additionally, I would like to thank Dr. Paul Lennard, who has been the most amazing teacher. He let me experience practical issues beyond the textbooks, patiently edited my writing, and encouraged me to follow my passions. I would also like to thank Dr. N. Wendell Todd, and Dean Wendy Newby for guiding

my research and helping me to develop my background in hearing loss and other impairments. Special thanks goes to Dr. Michael Crutcher and Nadia Brown for their support these past couple of years, especially during my participation in the NBB Honors Program.

I would like to acknowledge the Atlanta Neuroscience Education and Training Program (NET/work), which provided me with a two-year neuroscience immersion in research. They provided funding for my research (both at Emory and other partner institutions), great mentoring, and a network of local and national peers in neuroscience. I would like to thank Dr. Gabriel Corfas, who gave me the opportunity to conduct research in his lab at HMS in the summer of 2012; this is when I absolutely fell in love with Otolaryngology. My research would not have been possible without their support.

I would also like to thank my mother, Hyacinth Taylor. She is always supporting me and encouraging me with her best wishes. I am reluctant to name the friends, as I would certainly miss some. But, they have been an integral part of my primary and secondary school years. I am thankful to my extended family for standing by me and for keeping me grounded.

As a sophomore at North Miami Beach Senior High School (NMBSHS), I decided to enroll into American Sign Language (ASL). I had my reasons for doing so, mainly that I was afraid to take Spanish. But, ASL became much more than a class for me. At the time, NMBSHS was the only school in South Florida with a Deaf instructor teaching ASL to hearing students. This experience changed my perception of human disease, opening my eyes to the role that culture played in medicine. For

two years, I watched the hands of Ms. Cathy Oshrain, my amazing teacher, more intently than I had ever watched anything. I dedicate this thesis to her.

This study was supported by grants to Dr. Lin from the National Institute on Deafness and other Communication Disorders (NIDCD 4R33DC010476 and RO1 DC006483), and in part by a Technical Development grant from the Biomedical Imaging Technology Center at Emory University School of Medicine (TD011-9.4T).

Table of Contents

Introduction

Hearing loss is the most common sensory disability in the world, especially in developed countries and among aging populations. Although not life threatening, hearing impairment can be burdensome to one's social and professional life. Hearing loss is an etiologically heterogeneous trait with many known environmental and genetic causes such as premature birth, infections, noise exposure, and exposure to ototoxic drugs. Hearing loss is typically classified as conductive or sensorineural hearing loss (SNHL). Congenital hearing loss occurs when sound is not conducted efficiently through the outer ear canal to the eardrum and the ossicles of the middle ear, while SNHL occurs when there is damage to the inner ear, or to the nerve pathways from the inner ear to the brain. Additionally, hearing loss can be syndromic (associated with other symptoms) or nonsyndromic (occurring in isolation). There has been a rise in the proportion of hereditary hearing impairment compared to deafness from infective or environmental origin. Conductive impairment can be caused by otitis media, otosclerosis, or obstruction by a tumor or other foreign body and is often reversible. Bilateral congenital (from birth) SNHL affects one in every 500 newborns and may lead to significant problems in speech development, educational attainment, employment prospects, and life expectancy (Kochhar et al. 2007; Hildebrand et al. 2008). Presbycusis or age-related hearing loss is also common in developed societies, affecting 25- 40% of individuals over the age of 65. For patients with mild-to-moderate hearing loss, hearing aids can provide significant amplification. However, for severe-to-profound hearing loss (sensorineural) cochlear implantation is usually the better habilitation option

(Cullen et al., 2004). Despite the marked success of these interventions, better restoration of normal hearing function is still needed for a better outcome. One of the key requirements is to have a better diagnosis of inner ear structures under pathological conditions.

According to Hrabé (2006), the gold standard for morphological study of the cochlea is Araldite Embedding for Light Microscopy. As a harder embedding medium compared to paraffin wax, plastic resin allows better preservation of the tissue. However, it is difficult to obtain perfect histologic serial sections of the cochlea, even with the use of a suitable resin such as araldite. The chemical processing (i.e. demineralization of hard tissue) and mechanical stress (i.e. the act of sectioning) imparted on the sample during preparation, often compromises the original morphology (Hrabé, 2006, p. 9). Furthermore, histologic sections cannot be applied to living organisms. The difficulty of nondestructive morphologic observation of the elements of the auditory sensory organ in the bony labyrinth is one of the chief reasons why understanding of the underlying biology of inner ear diseases, and the establishment of therapy for them have been hindered (Shibata et al, 2009). There is a need for an efficient, non-invasive method to follow the morphological changes in genetically engineered deaf mice. We believe that the evaluation of patients with SNHL will be improved by the use of more accurate diagnostic techniques such as magnetic resonance imaging of the temporal bone, and two-photon micro-endoscopy.

Mice are excellent model organisms for studying hearing and deafness. Knockout and transgenic mice have enabled the study of Cx26 function in the inner

ear. An important point to mention, is that in contrast to human patients where homozygous loss-of-function mutations in GJB2 leads to non-syndromic hearing loss (NSHL), a complete knockout (KO) of Gjb2 in mice results in embryonic lethality (Sheffield, 2012). Thus, targeted (conditional) KOs are utilized to study Cx26 function. Currently, there are no reported studies involving the use of MRI to study morphological changes in cCX26 null mice, let alone connexin-associated hearing loss.

Overview of Sound Processing/Anatomy of the Mammalian Ear

The ear is responsible for translating variations in air pressure-whether from speech, music, or other sources-into neural activity necessary for our perception and interpretation of sound. Sound waves are first collected by the outer ear, which consists of the pinna (external ear) and external auditory meatus (ear canal). The shape and structure of the external ear amplifies the sound waves (particularly at the frequency ranges of 2,000 to 5,000 Hz, a range that is important for speech perception in humans) and focuses them upon the tympanic membrane (ear drum). The sound waves vibrate the eardrum, which in turn vibrates three tiny bones in the middle ear - the malleus (hammer), incus (anvil), and stapes (stirrup). The stapes vibrates a small membrane at the base of the cochlea, the oval window, which transmits amplified vibrational energy to the fluids within the cochlea. In mammals, the portion of the inner ear involved in audition is called the cochlea. It is a coiled structure, which is responsible for converting sounds into neural activity. The portion nearest to the oval window is the base of the cochlea, while the region at the top end of the coil is referred to as the apex. The other sensory component of the

inner ear is the vestibular system, which is responsible for balance. The vestibular system detects head position and motion. The three semicircular ducts detect angular acceleration and deceleration in all three planes. The utricle and saccule detect position of the head relative to gravity as well as changes in position. The cochlea, vestibule, and the semicircular canals (superior, posterior, and lateral) are encased in bone, making up the bony labyrinth. The membranous labyrinth is suspended within the bony labyrinth. The utricle and saccule in the vestibule, the three semicircular ducts located in the semicircular canals and the membranous duct of the cochlea make up the membranous labyrinth.

Along the length of the cochlea are three parallel canals: the tympanic canal (scala tympani), vestibular canal (scala vestibule), and middle canal (scala media or cochlear duct). The tympanic and vestibular canals are filled with a high-sodium containing fluid called perilymph. This perilymph is nearly identical to spinal fluid and differs significantly from the endolymph (high potassium-containing fluid), which fills the cochlear duct (Figure 1). Endolymph also surrounds the sensitive Organ of Corti, which is the sensory region of the cochlea that is chiefly responsible for converting sound into nerve impulses; it lies on the basilar membrane (Figure 1). The Organ of Corti consists of two types of cells: sensory hair cells and an elaborate framework of non-sensory supporting cells. The two types of sensory cells, the outer (OHC) and inner (IHC) hair cells, are arranged in ordered rows. Three rows of OHCs are located on the lateral edge, while a single row of IHCs is located on the medial edge of the organ of Corti. The mammalian organ of Corti contains at least seven distinct types of supporting cells (Figure 3): inner sulcus cells, pillar cells,

border/inner phalangeal cells, deiters cells, hensen cells, and Claudius cells (not shown). Supporting cells rest on the basilar membrane and provide support to the sensory hair cells. They are vital to the maintenance of cochlear homeostasis. Thus, loss of supporting cells eventually results in death of hair cells and spiral ganglion neurons.

Auditory nerve fibers terminate onto sensory hair cells, and carry signals up to central brain structures. At the tips of hair cells are stiff, hair-like structures called stereocilia. The heights of these stereocilia increase over the surface of the hair cell, forming an inclined plane. Atop the organ of Corti is the tectorial membrane, an acellular membrane connected to the spiral limbus. The stereocilia of the outer hair cells extend into indentations in the bottom of the tectorial membrane. Thus, when sound vibrations move through the fluids within the cochlea, this causes the displacement of the basilar membrane. This then shifts the positioning of the stereocilia in relation to the tectorial membrane. Depending on the direction that the stereocilia bend, ion channels within the hair cells will either open or close. This change in ion concentration within the hair cell either increase or decrease the firing rate of the auditory nerve fibers.

GJB2 (Cx26)

It is estimated that the mutation of any of several hundred gene may result in hearing impairment, which emphasizes the complexity of the inner ear and the array of proteins necessary for hearing. Currently around 100 deafness genes have been identified. Monogentic mutations in any one of these genes may cause hearing loss. Of the deafness mutations that have been identified, they have been found to

affect sensory hair cells (e.g. MYO7A, KCNQ4), the tectorial membrane (e.g. COL11A2, TECTA), and non-sensory supporting cells (e.g. GJB2, GJB6) (Van Camp and Smith, 2010, Kochhar et al., 2007, Petit and Hardelin, 2001). Mutations in Gap Junction Beta-2 (GJB2), classfied as DFNB1, are responsible for 30-50% of pre-lingual autosomal recessive inheritance (ARNSHL) cases in various populations (Petersen and Willems, 2006). The DFNB1 locus contains the deafness genes GJB2, which encodes connexin 26 (CX26), and GJB6 that encodes CX30 proteins (Kelsell et al., 1997; del Castillo et al., 2002).

Connexin 26 is a beta-2 gap junction protein. Different Cx protein subunits are conventionally named by adding a number that corresponds to their molecular weight (e.g., Cx26). Connexins (Cxs) are the building blocks of gap junctions (GJs), which are specialized membrane channels that allow the transport of ions and small molecules (molecular weight <1k dalton) necessary for cell signaling and homeostasis. Cxs are membrane proteins that consist of four trans-membrane domains. Six compatible Cx subunits form a complex (a hexamer), called a connexon (Figure 1B). Two hexamers in adjacent cells align to form a complete gap junction channel, which connects the cytoplasms of the cells involved when the channel is open. The Cx gene family comprises twenty members in the mouse and twenty-one members in the human genome (Willecke et al., 2002).

Cx26 Expression in the Inner Ear

Connexins are expressed in most tissues and tissues can express multiple connexin isoforms at one time. The inner ear expresses multiple connexin isoforms including CX26, CX29, CX30, CX31, and CX43 (Harris and Locke, 2009). CX26 and

CX30 are the most predominant Cx subunits in the cochlea. They are expressed between cells within the spiral ligament, interdental cells of the spiral limbus, and the supporting cells of the organ of Corti. CX26 and CX30 are co-expressed and form homo- (gap junction channel is formed by two identical connexons) and heterotypic (gap junction channel is formed by at least two different connexons) gap junction channels. These channels within the cochlea form two gap junction networks: the connective tissue network and the epithelial network. The connective tissue network is in the lateral wall between the basal and intermediate cells of the stria vascularis and fibrocytes of the spiral ligament, while the epithelial gap junction network connects the supporting cells of the sensory epithelia and bordering epithelial cells (Figure 2) (Kudo et al., 2003; Chen et al., 2005).

Cx26 Function in the Inner Ear

There is a paucity of information regarding the function of Cx26, but it is clear from human and mouse studies that CX26 and CX30 play a crucial role in cochlear development, maintenance of homeostasis and, ultimately, function. Cx26 is believed to play an important role in regulating potassium flow from hair cells in the Organ of Corti, buffering and recycling of K^+ following mechano-transduction by the sensory hair cells (Ortolano et al., 2008). However, experimental evidence directly supporting the K^+ recyclying hypothesis is lacking. In addition to K+, GJs have been shown to transport other signaling molecules such as ATP, cAMP, IP3 (Martinez et al., 2008; Nickel et al., 2008) and glucose (Chang et al., 2008). It's been proposed that connexons play a role in maintaining osmotic balance in the stria vascularis. Findings from cCx26 null mouse model indicate that Cx26 play critical

rols in the maturation of the morphology of the organ of Corti before the formation of the endolymphatic potential (Wang et al., 2009). Since the endolymphatic K^+ is low at the developmental stage, this observation demonstrates a critical developmental role for Cx26 before the K^+ recycling is required.

Conditional Cx26 (cCx26) Null Mouse Model and Cochlear Development

Previous work by the Lin lab centered on three different conditional knockout mice models, foxg1-Cre, pax2- Cre, and TMX-inducible, to study the role of Cx26 in the inner ear (Sun et al., 2009; Wang et al., 2009). A 40-50 dB loss in hearing as well as impaired postnatal development of the organ of Corti was observed in these mice. Significant morphological observations include: failure to form the tunnel of Corti (or space of Nuel), degeneration of Claudius cells at postnatal day (P) 8, and loss of outer hair cells and supporting cells at approximately P13. Cellular apoptosis started in the middle cochlear turn, eventually extending to apical and basal turns of the cochlea. Complete degeneration of the organ of Corti in the middle turn was observed by one month of age. These mice indicate that Cx26 plays an important role in the development of the organ to Corti prior to the onset of hearing (approximately at P14). Results of these studies suggest that developmental abnormalities of the cochlea precede cellular death (Wang et al., 2009).

Magnetic Resonance Imaging

Magnetic Resonance Imaging (MRI) is a technique traditionally used for structural analysis (to visualize internal structures of an organism's body in detail) in the field of medicine. It is now becoming more and more useful in the

neurosciences as both an anatomical and functional localization tool, serving in place of histological studies for identification of areas in the body.

MRI makes use of the property of nuclear magnetic resonance (NMR) to image nuclei inside the body. In Figure 3, an illustrated description of MRI is provided. The MRI scanner is typically a large, U-shaped magnet, which creates an external magnetic field. When placed into this strong magnetic field, the unpaired nuclear spins align with the field. This forms a net magnetization vector parallel to the magnetic field. At its core, NMR utilizes the absorption and emission of radiofrequency electromagnetic radiation (RF) by nuclei. In response to RF pulses that match the Larmor frequency of hydrogen atoms (which is the likely target due to the abundance of water in the body), there is absorption of energy by the spins, leading to a change in orientation of the magnetization vector. The spins eventually release this energy and revert to their original orientation (or equilibrium), a process called relaxation. T1 (longitudinal) and T2 (transverse) relaxation are the two types of relaxation commonly measured by MRI. T1 relaxation is due to spin-lattice interactions, or the transfer of energy from inverted susceptible nuclei to the surrounding lattice (or milieu). These nuclei relax back into a lower energy state, or in others words, gradually realign with the direction of the applied magnetic field. T2 relaxation is due to spin-spin interactions, where energy is directly transferred between two susceptible nuclei of similar precession frequencies. No net change in T1 is observed, as the spins only reverse orientation relative to the field created by the external magnet. There is a loss of phase coherence when the transfer occurs, resulting in a drop in T2. The MRI scanner detects these relations, and translates

them into MRI signal. This is possible because the differences in tissue composition significantly impacts relaxation parameters. Capturing these differences is key to create MRI contrasts (Massoud and Gambhir, 2003).

There are many benefits to the use of MRI. It has no well documented limit of tissue penetration, has good spatial resolution and tissue contrast, and has the potential to combine anatomical, functional (fMRI) and molecular imaging (Hoehn et al., 2008). It does not require radioactive probes (like PET imaging), and this can be performed repeatedly on most patients. MRI is significantly less expensive than PET and CT imaging, and unlike CT, MRI uses no ionizing radiation. Additionally, the contrast agents used in MRI are less likely to cause an allergic reaction, compared to the iodinated contrast agents used in CT. Furthermore, more MRI scanners are available due to its clinical relevance.

Magnetic resonance imaging (MRI) has recently emerged as one of the most predominant imaging techniques for visualization of the internal structures of opaque specimens (typically bone) with classical histological-like quality. This technique has been proven very useful in Otology, allowing the acquisition of high-resolution images at 4.7T and 9.4T. T1 contrast-agent-enhanced MRI has been use to investigate inner ear pathology in various animal models and human patients. Using gadodiamide, a gadolinium derivative, imaging of guinea pig cochleae was made possible. Researchers were able to demonstrate normal and impaired function of the barriers within the inner ear, delineating the basal, medial and apical scala tympani (ST) and scala vestibule (SV) successfully (Counter et al. 2000). Furthermore, other MRI studies of guinea pigs have addressed the possible origins

of perilymph, which fills the ST and SV, as well as Possible origins of perilymph, pathological changes in endolymphatic hydrops and perilymphatic fistulae (Pyykko et al. 2010; Zou et al., 2003, 2005, 2009a, 2009b). Additionally, in the study of Meniere's disease, MRI has proved useful for observation of cochlear and vestibular endolymphatic hydrops in humans (Naganawa et al. 2008, Nakashima et al. 2007). Perhaps the most impressive report is that of a high-resolution MRI study of the human inner ear by Silver et al. 2002. The group reported magnetic resonance imaging scans of a fresh human cochlea at 23 and 46 μm resolution, using a 256 x 256 x 256 acquisition matrix. The images revealed detailed anatomy of the modiolus, utricle, saccule, semicircular canals, and facial nerve (which are among the most commonly reported inner ear structures successfully delineated through MRI examination). Additionally, they were able to identify intracochlear structures such as the osseous spiral lamina, Reissner's membrane, membranous spiral lamina, and spiral ligament. In this work we plan to image mouse cochlea, which is considerably smaller than the human and guinea pig cochlea.

Methods

Animal Groups and Sample Preparation

All animals used in this study were treated humanely following a procedure approved by the Institutional Animal Care and Use Committee at Emory University. Animal groups consisted of either Foxg1-Cre Cx26 null or littermate-matched wild type (WT) mice, which were provided by the lab of Dr. X. Erick Lin at Emory University. The cCx26 null mouse model were generated by cross breeding two

kinds of genetically-engineered mice:

1. Mice expressing the DNA recombinase Cre in the cochlea but not in the placenta. One of the two *Foxg1* alleles of these mice has been replaced with the Cre recombinase gene. Heterozygous *foxg1cre/+* mice were originally obtained from the Jackson Laboratories (Bar Harbor, ME). *foxg1Cre/+* mice show normal hearing (Wang et al., 2001).

2. Mice in which the exon2 of the target gene, *Gjb2*, is modified by the insertion of two loxP sites that enable activated Cre recombinase to excise the flanked (floxed) gene segment. The Gjb2 gene is flanked by the loxP sequence (Cx26loxP/loxP mice). The exon2 of the *Gjb2* contains the entire coding region for the Cx26. Thus, activation of Cre recombinase is expected to totally remove the expression of Cx26. The Cx26loxP/loxP breeding pairs were obtained from the European mouse mutant archive (http://www.emmanet.org/) with the written permission of Dr. Claus Willecke. Previous studies show that the hearing of Cx26loxP/loxP mice is normal (Cohen-Salmon et al., 2002).

Cardio-perfusion with 4% paraformaldehyde was performed on all animals. Post-fixation, the head of each mouse was removed for experimental use. We submitted these samples for micro-MR Imaging, and evaluated the quality of the collected images. In order to compare to the images obtained by traditional histological method, we then obtained epoxy resin cochlear sections for optical imaging, which were then used to compare our findings using micro-MRI (Figure 4). Details about resin cochlear sectioning experimental protocol are given in the

following sections.

Magnetic Resonance Imagining Experiments

All MRI image data were collected on a BioSpec 9.4 T spectrometer (Bruker BisoSpec 94/20, Karlsruhe, Germany) equipped with 1000 mT/m actively shielded gradients. A radio frequency (r.f.) volume coil with 35 mm inner diameter was used for both transmit and receive. Data were acquired with a 3D fast spin-echo sequence and the following parameters: TR (repetition time)/ TE_{eff} (effective echo time) = 1500/45 msec, FOV (field of view) = 20.3×16.8×4.2 mm^3, matrix size = 290×240×48, resulting in a resolution of 70×70×70 μm^3, rapid acquisition with relaxation enhancement (RARE) factor = 8, and 24 average. Analysis was performed using the ParaVision 4.0 software package (Bruker BioSpec, Karlsruhe, Germany).

Morphological Study

Four mouse bullae were processed for Araldite embedding after MRI measurements to show gross anatomic comparison between MRI and histology. For obtaining epoxy resin cochlear sections, we fixed cochleae first through cardio-perfusion of 4% paraformaldehyde (in PBS). The cochlea was dissected out and post-fixed in 1% osmium overnight at room temperature. Samples were decalcified in 0.35 M EDTA (pH 7.5, in PBS) for 72 hours at 4°C, followed by gradual dehydration in alcohol of increasing grades (35%, 70%, 90%, and 95% ethanol for 30 minutes each, and absolute ethanol twice for 30 minutes), infiltrated, and embedded in epoxy resin with the conventional protocols. Consecutive cochlear sections (7 μm in thickness) were made with a glass knife on a microtone section machine (cut with a Leica CM1850, Germany) and were stained with toluidine blue. The slides were observed

under light microscope and digitally photographed (Zeiss Axiovert 135 microscope and Zeiss Axiovision 3). Final figures were compiled and analyzed analyzed by Image J software package (NIH, http://rsbweb.nih.gov/ij/ features.html). The brightness and contrast of some of the image panels were adjusted for better clarity. No other photo manipulations were done to enhance the pictures.

Results

Cochlear sections obtained from normal and cCx26 null mice cut from two-month old animals were compared. In the cCx26 null mouse, we observed flattening of the epithelium stretching between the inner sulcus and the outer sulcus (Figure 5). Specifically, in the organ of Corti there was loss of both outer and inner hair cells in the middle and basal turn (not shown), and supporting cells surrounding outer hair cells (including inner sulcus cells, pillar cells, border/inner phalangeal cells, deiters cells, hensen cells, and Claudius cells).

In regards to the MRI experiment, lymph detection did enable the visualization of some internal ear sub-regions composed of bones, cartilage and membrane, as well as the cochlear anatomy. Long duration micro imaging experiments were performed to record the details of the mouse ears available at 9.4T in the heterogeneous regions of the ear. Image processing by 2D analysis was performed. An image with an in plane resolution of 70μm allowed to delineate main inner ear components such as the cochlea, utricle, saccule, and semicircular canals (Figure 6.1). The T1-weighted sequences showed that the perilymph, which filled the scala tympani, scala vestibule, and vestibulum generated a bright signal. Where

as endolymph, which filled the scala media and ampullae of the semicircular canals were dark (Figure 6.2). Thus, the scala tympani and vestibuli were distinguishable from the scala media. We were able to approximate the location of the cochlear aquaduct, which is adjacent to the scala tympani and of similar intensity, and the lateral wall. Additionally, we identified structures within the cochlea such as the osseous spiral lamina and helicotrema (Figures 6.1 and 6.4), and modiolus (Figure 6.3). The modiolus showed grey signal (bright, although less so than the perilymph) while the osseous spiral lamina was dark. Bone appears black in a T1-weighted image.

Improved image quality was found for high-power evaluation of osmium-stained plastic-embedded, serial sections compared to MRI sections. In the plastic section we were able to observe the near complete degeneration of the organ of Corti in the cCx26 null mouse. Resutls showed complete degeneration of auditory sensory cells, supporting cells, neurons and other structures adjacent to the sensory epithelia. However, in the MRI scan of the cCx26 null mouse we can only make approximations about the location of such cells, relying on differentiation of bone, and fluid. We were not able to differentiate between the cellular structure and the fluid surrounding it.

Discussion

The gold standard: Plastic sectioning

We were interested in assessing the loss of sensory hair cells and degeneration of SGNs in the cochlea of conditional Cx26 null mice when Cx26

expression is significantly reduced. We wanted to use the resin sections as a reference for what might be expected in the cochlea upon MRI observation. Meniere's disease is an inner ear disorder that has been better understood through the comparison of classical resin sections and MRI sections. Cochlear resin sections of a Meniere's disease patient often demonstrate abnormalities in the membranes that contain perilymph and endolymph. As a result, there is an increase of signal intensity in the ST, SV, SM, and semicircular canals. There are no previous studies that have compared these two imagining techniques to understand connexin-associated hearing loss.

Serial-section plastic-embedded material is a useful complement to the magnetic resonance images for several reasons: 1) one set of roughly 50 sections can be rapidly cut and mounted and contains the entire cochlear spiral; 2) the material is fixed, stained and embedded as if for electron microscopy, and thus has the highest quality of preservation, allowing high-power evaluation that can reveal subtle abnormalities in remaining hair cells, supporting cells, neurons and other structures adjacent to the sensory epithelia, including the stria vascularis, spiral ligament, dark cells, etc.; and 3) the cell bodies and peripheral axons of SGNs can be easily evaluated both qualitatively and quantitatively as has been shown in the previous publications (Sun et al. 2009; Zilberstein et al., 2012).

MRI: Is it good enough for cellular diagnosis?

Traditional MRI has proved useful in the clinical diagnosis of various disorders of the temporal bone and cerebellopontine angle, such as immune and viral labyrinthitis, multiple sclerosis, and schwannoma (Silver et al. 2002). MRI is

neither sensitive nor specific enough for diagnosing sensorineural hearing loss. However, based on our results it seems that the role of MRI in the mouse models of human connexin mutations associated hearing loss remains limited due to the spatial resolution attainable using currently available scanners. It was difficult to appreciate the membranes that contain the endolymph of the inner ear (where the organ of Corti lies) imaging *ex vivo* at 9.4T.

Our preliminary *in vitro* studies of mouse cochlea and vestibular organs has shown that, through using high-resolution MRI technologies, it is possible to visualize some inner ear anatomy. Although, not at a resolution comparable to osmium-stained plastic-embedded, serial sections (the gold standard for morphological studies). We were able to achieve a spatial resolution of 70 μm using high-resolution micro-MRI, but could not further improve the attainable voxel size, as increasing the acquisition matrix two dimensions would have greatly increased scanning time. Increasing spatial resolution may have allowed for better visualization of membranous architecture. In contrast to our results, Silver et al. (2002), using 9.4-Tesla high- resolution MRI, were able to achieve a resolution of 23 μm in human. Although impressive, this resolution was not sufficient to visualize individual cells.

Our conclusion is that, comparing to resin cochlear section method, magnetic resonance microscopy offer few advantages for use in studying the animal models of genetic deafness associated with connexin-associated hearing disorders, as MRI scans have insufficient resolution to visualize intracochlear cells. In this study samples were collected following the sacrifice of the study animal, and the temporal

bone core was exposed, which makes it difficult to make the transition to in vivo imaging.

Signal-to-Noise Ratio (SNR)

A high SNR is desirable in MRI. The SNR is dependent on the following parameters: slice thickness and receiver bandwidth , field of view, size of the (image) matrix , number of acquisitions , scan parameters (TR, TE, flip angle) , magnetic field strength , and selection of the transmit and receive coil (RF coil). Most important of these factors are field of view and the size of the image. The mouse cochlea is quite small, measuring at about 2.5mm. In order to encompass a maximum of picture elements (produce an image of high resolution), the matrix should be as large as possible. However, minimum pixel size is limited by the fact that SNR decreases with the size of the voxel. Furthermore, magnetic susceptibility to the multiple bone–fluid and air–fluid interfaces within the mouse (and human) temporal bone poses challenges through artifact and a decrease in the SNR (Silver et al. 2002). Additionally, the chosen resolution is a compromise between quality and time. In order to obtain a greater signal-to-noise ratio, measuring time (image acquisition or scan time) needs to be increased. Scan time is the key to the economic efficiency of the MR system. Furthermore, increased scan time is associated with reduced comfort (of the small animal, and ultimately of the human patient), and an increased risk for a displacement of the head during the high-resolution measurement. This practical limitation makes the high-resolution MRI imaging of live mouse difficult. The primary reason for not studying anaesthetized animals is that greater scan time is required (>15 hours) in order to acquire high-resolution

images. Although reporting an approximate scanning time of 12 hours, Silver et al. (2002), was able to achieve better resolution than 70 microns. The rare sequence employed in this study was comparable to our methodology (FOV (field of view) = 2.5 × 2.2 × 3.0 cm, TR/TE (times repetition/ times echo) = 35 ms/3 ms, NEX (number of exotations) = 20, matrix = 256 × 256 × 256. The resulting voxel size was 0.098 × 0.086 × 0.12 mm). Thus, the differing element was the use of a contrast agent.

The use of contrast agents

Commonly used, non-toxic, non-allergenic contrast agents can be for tissue enhancement, enabling the production of high-resolution magnetic resonance images of inner ear ultrastructure. The most commonly used of these agents are gadolinium-based. It has been used in mouse, rat, guinea pig, and human patients for in vivo imaging. Additionally, mercuric salts have been used to enhance Reissner's membrane. Although efficient, this preparation poses a great risk of toxicity for use in *in vivo* human studies.

Further more, it is possible that the contrast agent could leak through the tight junctions in the stria. We did complete a MRI scan in which Gd+++ was used, however the MRI image that resulted was not of improved quality. It is possible that this observation was due to leakage. This would result in excessive uptake of the contrast agent in the scala media, making it difficult to observe inner ear membranous structures (poor contrast differentiation). Furthermore, there is no consensus in the literature regarding the most effective route of delivery; previously reported administration routes include: intratympanic delivery, intravenous (IV)

delivery, via the oval window, and via the round window. The debate of local versus IV delivery is very important for future in vivo studies both in small animal and human. The passage of contrast agents through the normal blood perilymph barrier needs to be enhanced to achieve sufficiently high signal-to- noise ratio on MRI to enable visualization of the inner ear compartments.

Other Imaging Methods as alternatives

So far we've discussed the advantages and limitations of MRI and other common scans. As a result of insufficient resolution to establish cellular diagnosis, therapeutics for SNHL are undeveloped and generalized (limited to hearing aids and cochlear implants). The cochlea's small size, narrow chambers, and encasement in bone, has made it difficult to image the cells within. Optical techniques have emerged as a way to image intracochlear structures, as it provides a significantly higher spatial resolution and costs less than MRI and CT scans.

Confocal fluorescence microscopy is one such optical technique that has been applied to the cochlea (MacDonald and Rubel, 2008). Confocal microscopy although offering high resolution and deep penetration depth, relies on the use of exogenous labeling. Similar to the disadvantageous of araldite-embedding tissues, the exogenous dyes or antibodies may result in tissue deformation and artifacts, which limits the interpretation of results.

A new study employed a relatively new non-linear optical technique, two-photon excitation fluorescence (TPEF) microscopy, which provides a much deeper penetration, reduced photo-damage, and improved detection sensitivity while maintaining a spatial resolution comparable with confocal microscopy. TPEF has

proved very useful in medicine, as a means to image brain tissue, lymph nodes, blood flow, and now to image inside cochlear tissues (Yang et al. 2013). In the study, collaboration between Harvard Medical School/ Massachusetts Eye and Ear Infirmary and Cal-Tech, it was demonstrated that TPEF through the round window offered high-quality images of intracochlear cells, including sensory hair cells and cochlear neurons. The round window offers access to the cochlea through the middle ear. It's important to note that most cases of hearing loss (including noise-induced, ototoxic drug induced, and age-related) begins and is most severe in the region of the cochlea nearest to the round window.

There was no use of exogenous dyes nor was the cochlea opened in this study. In order to create an image, a near infrared laser was used as the source of excitation, and endogenous TPEF and second harmonic generation (SHG) was used for contrast. For the first time, images have been reported that reveal tissue structures within the cochlea at cellular level resolution with excellent SNR. These findings are important because they motivate the development of micro-endoscopes that will be able to form complete image from within the small and narrow cochlear chambers via the round window. Furthermore, the use of TPEF microscopy is likely to make its way into clinics soon to image human cochlea in vivo, as strategies straying away from the use of exogenous fluorescent dyes and transgenic fluorescent proteins are favorable. Being able to provide hearing-impaired patients with the highest level of care is of chief importance. In the future, imaging of these patients would allow in vivo evaluation of cochlear pathology to choose the most appropriate regenerative therapy targeted at specific cells that are missing in a

given patient. This study will facilitate the development of cochlea implants improved to avoid cellular trauma, enhance the performance of implants, and better monitor the delivery of therapies through these devices. In summation, optical imaging techniques render MRI obsolete and are a big step forward towards personalized medicine.

References

Ahmad S, Chen S, Sun J, Lin X. (2003). Connexins 26 and 30 are co-assembled to form gap junctions in the cochlea of mice. Biochem Biophys Res Commun. 307(2):362–368.

Hrabé, D. A., Chambon, P., & Brown, S. D. (2006). *Standards of mouse model phenotyping*. Weinheim: Wiley-VCH.

Chen, Y., et al. (2005). Mechanism of the defect in gap-junctional communication by expression of a connexin 26 mutant associated with dominant deafness. Faseb J. 19(11): p. 1516-8.

Counter SA, Bjelke B, Borg E, et al (2000). Magnetic resonance imaging of the membranous labyrinth during in vivo gadolinium (Gd- DTPA-BMA) uptake in the normal and lesioned cochlea. Neuroreport. 11:3979– 3983.

del Castillo, I., et al. (2002). A deletion involving the connexin 30 gene in nonsyndromic hearing impairment. N Engl J Med. 346(4): p. 243-9.

Harris, A.L. and D. Locke, eds. (2009). Connexins: A Guide. Humana Press: New York, NY.

Hildebrand, M.S., et al. (2007). Advances in molecular and cellular therapies for

hearing loss. Mol Ther. 16(2): p. 224-36.

Hoehn M, Himmelreich U, Kruttwig K, Wiedermann D. (2008). Molecular and cellular MR imaging: potentials and challenges for neurological applications. J Magn Reson Imaging. 27 (5):941-54.

Kelsell, D.P., et al. (1997). Connexin 26 mutations in hereditary non-syndromic sensorineural deafness. Nature. 387(6628): 80-3.

Kochhar, A., M.S. Hildebrand, and R.J. Smith. (2007). Clinical aspects of hereditary hearing loss. Genet Med. 9(7): p. 393-408.

Kudo, T., et al. (2003). Transgenic expression of a dominant-negative connexin26 causes degeneration of the organ of Corti and non-syndromic deafness. Hum Mol Genet. 12(9): p. 995-1004.

Liang C, Zhu Y, Zong L, Lu GJ, Zhao HB. (2012). Cell degeneration is not a primary causer for Connexin26 (GJB2) deficiency associated hearing loss. Neurosci Lett.18;528(1):36-41.

MacDonald GH and Rubel EW. (2008). "Three-dimensional imaging of the intact mouse cochlea by fluorescent laser scanning confocal micro- scopy," Hear. Res. 243(1–2), 1–10.

Martinez, A.D., et al. (2008). Gap-junction channels dysfunction in deafness and hearing loss. Antioxid Redox Signal. 11(2): p. 309-22.

Massoud TF and Gambhir SS. (2003). Molecular imaging in living subjects: seeing fundamental biological processes in a new light. Genes & Dev. 2003. 17: 545-580

Naganawa S, Sugiura M, Kawamura M, et al (2008). Imaging of endolymphatic and

perilymphatic fluid at 3T after intratympanic administration of gadolinium-diethylene-triamine pentaacetic acid. AJNR Am J Neuroradiol. 29:724–726.

Nakashima T, Naganawa S, Sugiura M, et al. (2007).Visualization of endolymphatic hydrops in patients with Meniere's disease. Laryngo- scope. 117:415–420.

Nickel, R. and A. Forge (2008). Gap junctions and connexins in the inner ear: their roles in homeostasis and deafness. Curr Opin Otolaryngol Head Neck Surg. 16(5): p. 452-7.

Ortolano, S., et al. (2008). Coordinated control of connexin 26 and connexin 30 at the regulatory and functional level in the inner ear. Proc Natl Acad Sci U S A. 105(48): p. 18776-81.

Petit, C., J. Levilliers, and J.P. Hardelin, Molecular genetics of hearing loss. Annu Rev Genet, 2001. 35: p. 589-646.

Petersen, M.B. and P.J. Willems, Non-syndromic, autosomal-recessive deafness. Clin Genet, 2006. 69(5): p. 371-92.

Postnov A, Zarowski A, De Clerck N, Vanpoucke F, Offeciers F, Vandyck D, Peeters S. (2006). High resolution micro-CT scanning as an innovatory tool for evaluation of the surgical positioning of cochlear implant electrodes. Acta Oto-Laryngologica. Preview: 1-8

Pyykko I, Zou J, Poe D, et al (2010). Magnetic resonance imaging of the inner ear in Meniere's disease. Otolaryngol Clin North Am. 43:1059–1080.

RJH Smith, GE Green, G Van Camp. Nonsyndromic Hearing Loss and Deafness, DFNB1. GeneReviews at GeneTests: Medical Genetics Information Resource

[database online] Available from http://www.geneclinics.org/ (accessed September 10, 2012)

Sun J, Ahmad S, Chen S, Tang W, Zhang Y, Chen P, Lin X. (2005). Cochlear gap junctions coassembled from Cx26 and 30 show faster intercellular Ca2+ signaling than homomeric counterparts. Am J Physiol Cell Physiol. 288(3):C613–C623.

Teubner B, Michel V, Pesch J, Lautermann J, Cohen-Salmon M, Sohl G, Jahnke K, Winterhager E, Herberhold C, Hardelin JP, Petit C, Willecke K. (2008). Connexin30 (Gjb6)-deficiency causes severe hearing impairment and lack of endocochlear potential. Human molecular genetics. 12(1):13–21.

Van Camp, G., Smith, R.J.H., Hereditary Hearing Loss Homepage, 2010.

Wang, Y., et al. (2009). Targeted connexin26 ablation arrests postnatal development of the organ of Corti. Biochem Biophys Res Commun. 385(1): p. 33-7.

Zou J, Pyykko I, Bretlau P, et al. (2003). In vivo visualization of endolymphatic hydrops in guinea pigs: magnetic resonance imaging evalua- tion at 4.7 Tesla. Ann Otol Rhinol Laryngol. 112:1059–1065.

Zou J, Pyykko I, Bjelke B, et al (2005). Communication between the perilymphatic scalae and spiral ligament visualized by in vivo MRI. Audiol Neurootol. 10:145–152.

Zou J, Zhang W, Poe D, et al (2009a). Differential passage of gadolinium through the mouse inner ear barriers evaluated with 4.7 T MRI. Hear Res. 259:36–43.

Zou J, Poe D, Bjelke B, et al (2009b). Visualization of inner ear disorders with MRI in vivo: from animal models to human application. Acta Otolaryngol Suppl.

560:22–31.

Figures

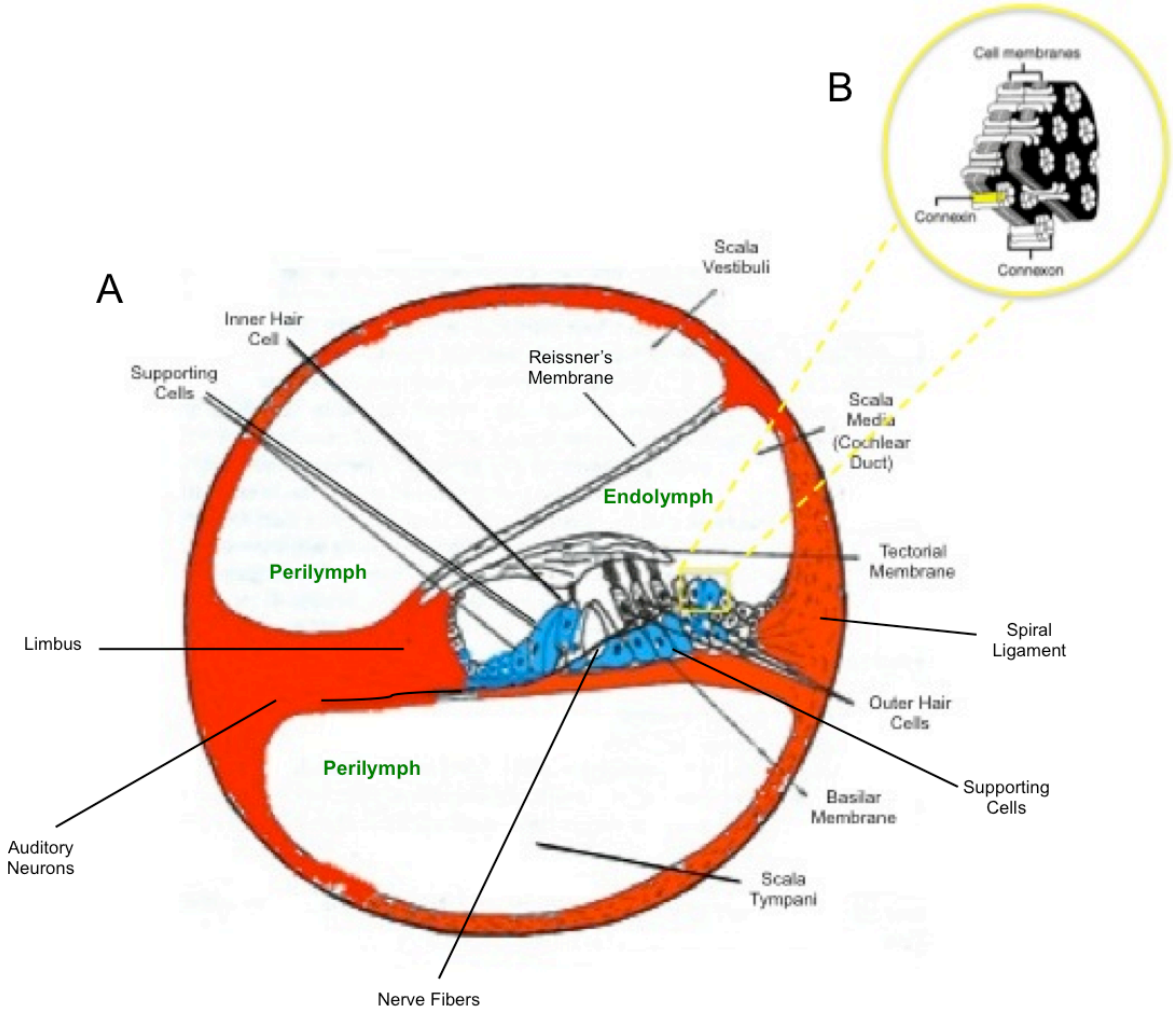

Figure 1. Cross-section of a cochlear turn. A: The the collective term for the sensory elements involves in sound transduction, lies on the flexible basilar membrane. It is surrounded by large fluid spaces (scala vestibule and scala tympani). The organ of Corti contains sensory cells (inner and outer hair cells) that respond to pressure waves in the fluid spaces by releasing neurotransmitter from their bases, increasing or decreasing neuronal firing rate. The nerve fibers that terminate on the hair cell bases are extensions of the auditory neurons. Endolymph fills the Cochlear Duct, while perilymph fills the Scala Vestibuli and Scala Tympani. B: Each connexin 26 molecule is known as a connexin (yellow). Six connexins oligomerize to form a connexon, and each connexon joins with another to form a gap junction. Adapted from Hildebrand et al. 2007 and Sheffield, 2012.

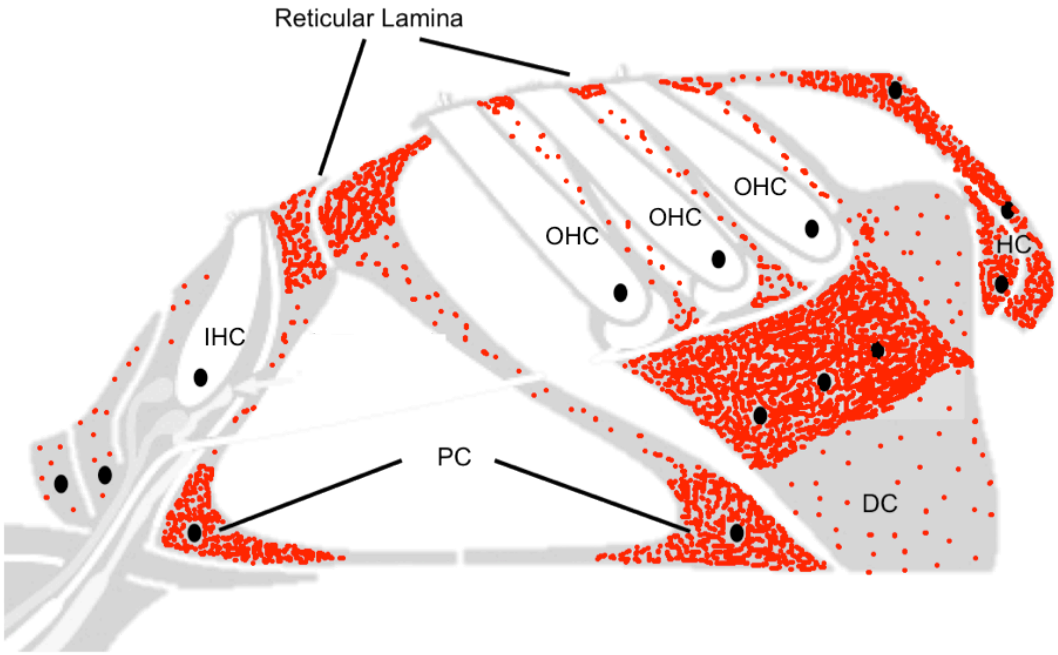

Figure 2. Cx26 Expression in the Organ of Corti. Cx26 is expressed in the nonsensory epithelial cells (interdental cells of the spiral limbus, inner and outer sulcus cells, sensory supporting cells, and cells within the root process of the spiral ligament), and the connective tissue cell system (fibrocytes of the spiral ligament and spiral limbus, basal and intermediate cells of the stria vascularis) shown in red. Abbreviations: IHC: Inner Hair Cell, OHC: Outer Hair Cell, Pc: Pillar Cell, DC: Deiter Cell, Hc: Hensen Cell. Adapted from art by Anne Luebke, University of Rochester Medical Center

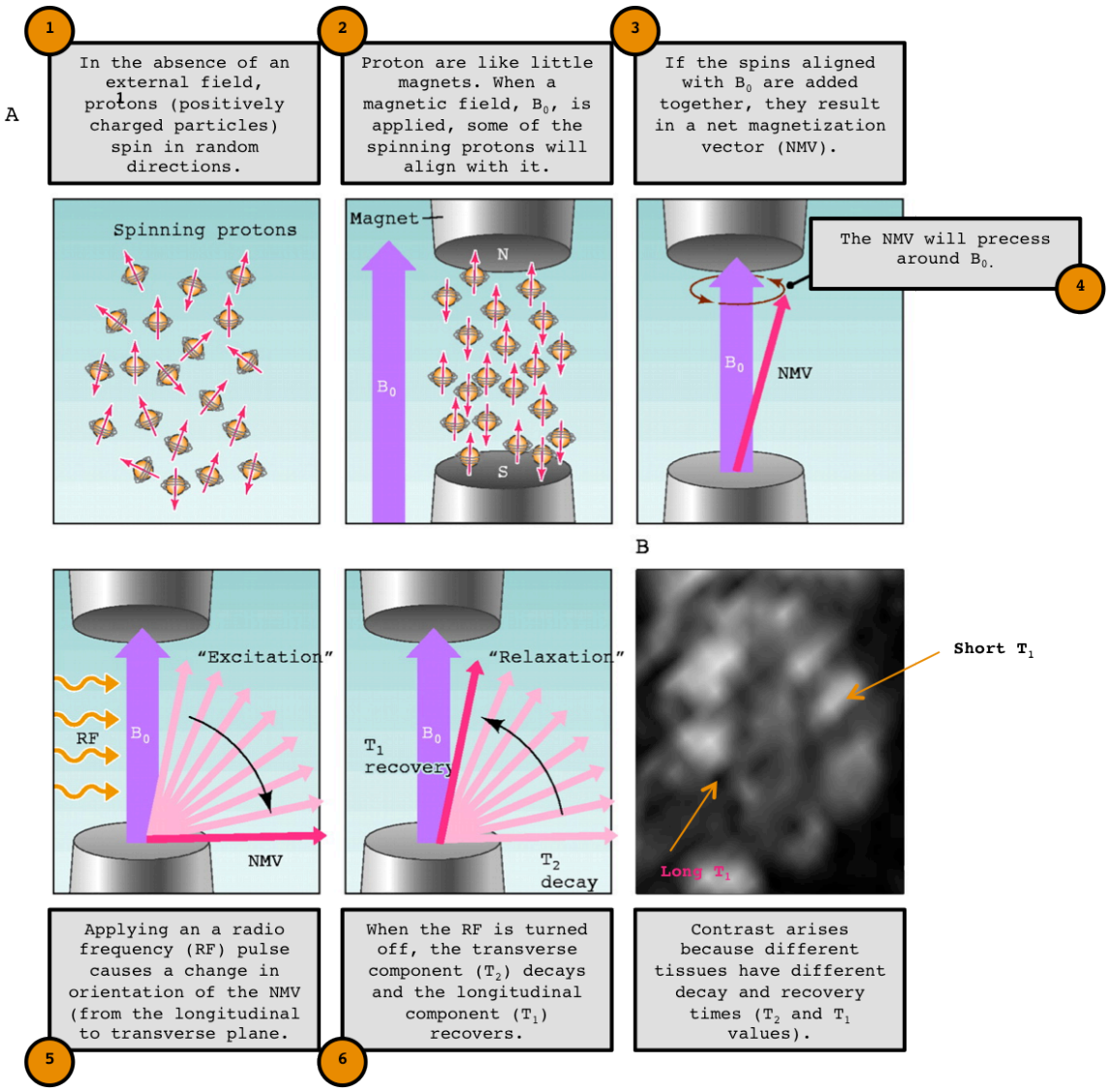

Figure 3. Description of magnetic resonance imaging (MRI). The steps in the MRI process (A). Cochlear section that illustrates contrast arising from different T_1 values. In a T_1-weighted MRI image, tissues with a shorter T_1 will have a higher signal intensity than tissues with a longer T_1. Adapted from Pautler et al. 2004.

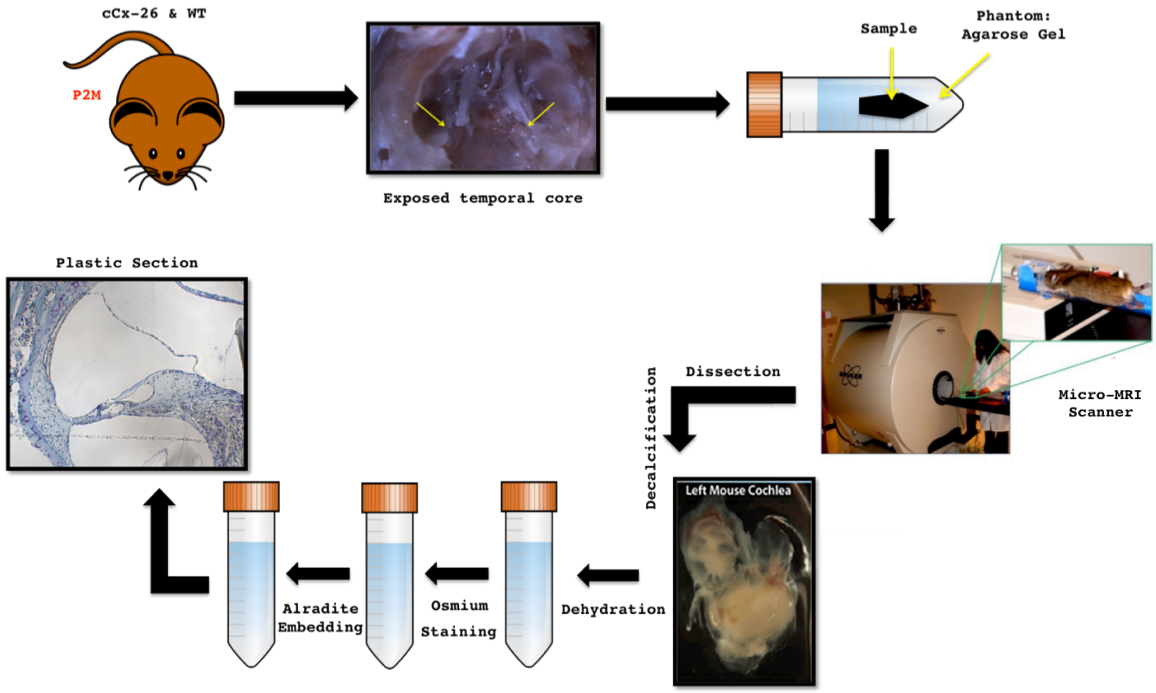

Figure 4. Schematic of research methodology.

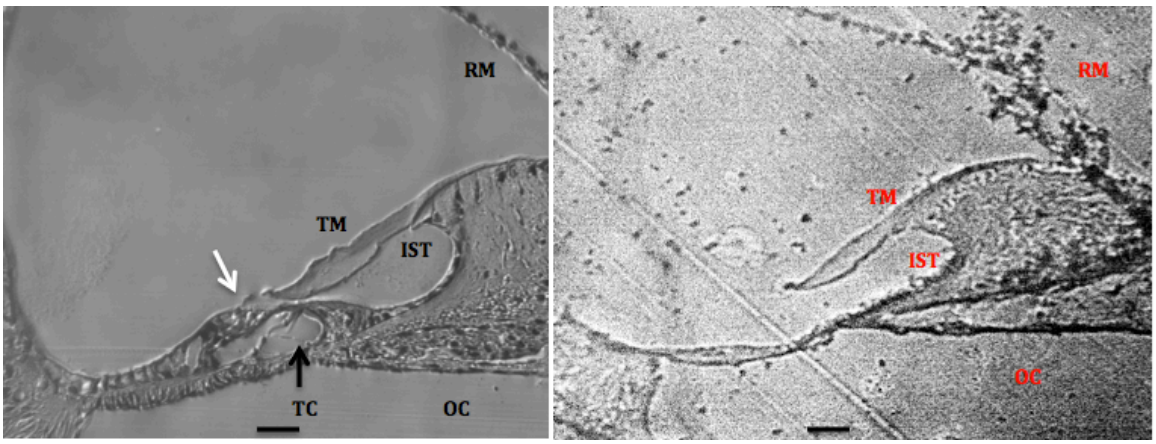

Figure 5. Histological analysis of the cochlea from normal mouse (a) and cCx26 KO mouse (b) at ~ 2 months of age. In cCx26 null mouse the organ of Corti has degenerated, leaving a flattened epithelium stretching between the inner sulcus and the outer sulcus (small yellow arrows). Abbreviations: TC: Tunnel of Corti; TM: tectorial membrane; IST: Inner Spiral Tunnel, OC: Organ of Corti, RM: Reissner's Membrane. The white arrow points to sensory hair cells of the Organ of Corti. Scales represent approximately 100 µm. The image for the normal mouse was provided by Dr. Kim.

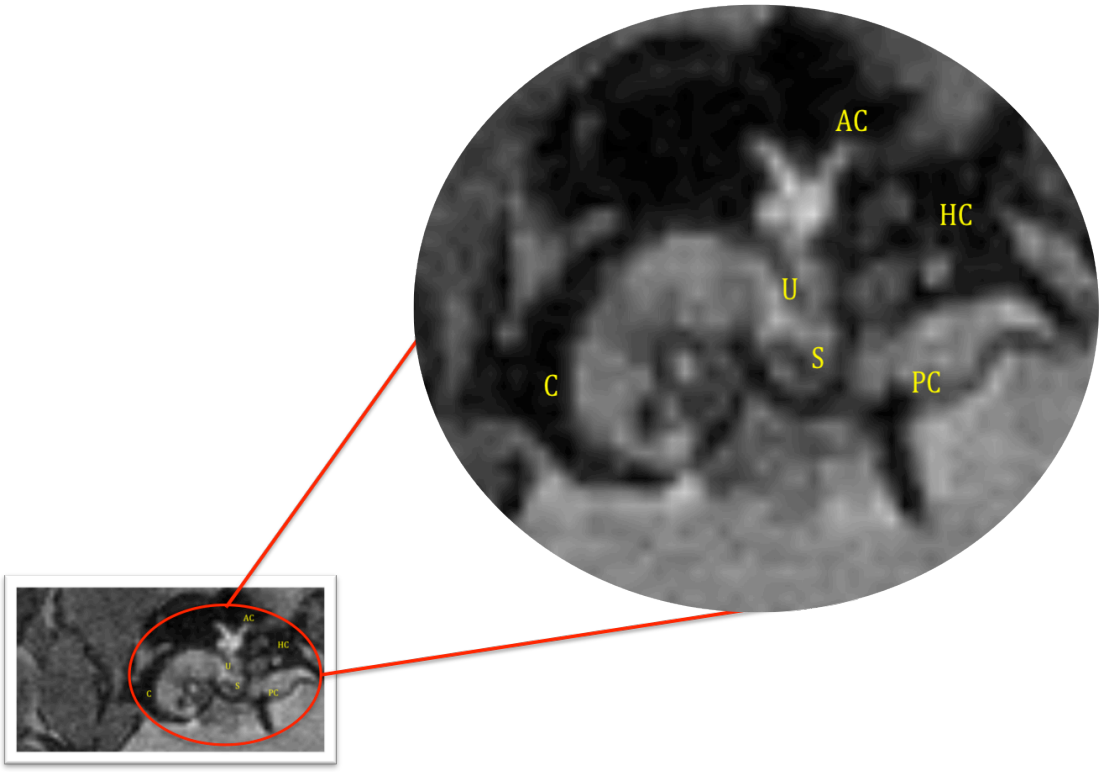

Figure 6.1. Coronal sections of Cochlea. A T1-weighted image; Resolution is 77×77×77 µm3. Abbreviations: AC: Anterior Canal, HC: Horizontal Canal, PC: Posterior Canal, U: Utricle, S: Saccule, C: Cochlea

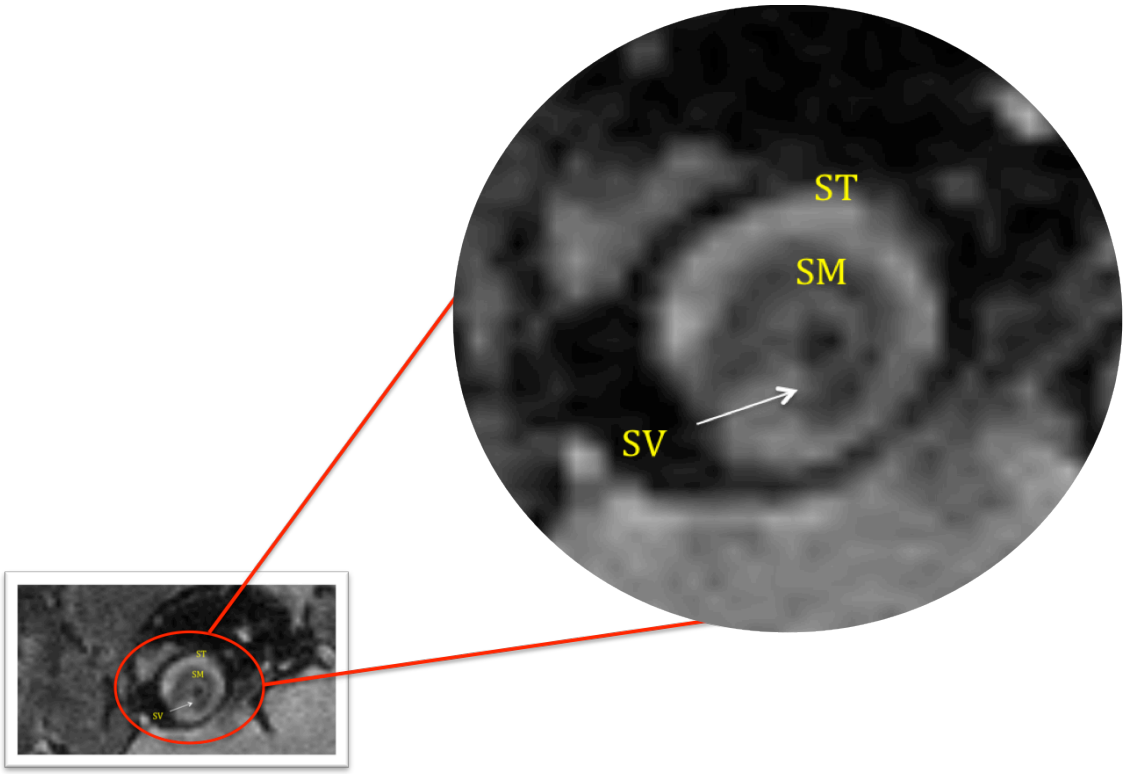

Figure 6.2. Coronal sections of Cochlea. A T1-weighted image; Resolution is 77×77×77 µm3. Abbreviations: ST: Scala Tympani, SM: Scala Media, SV: Scala Vascularis.

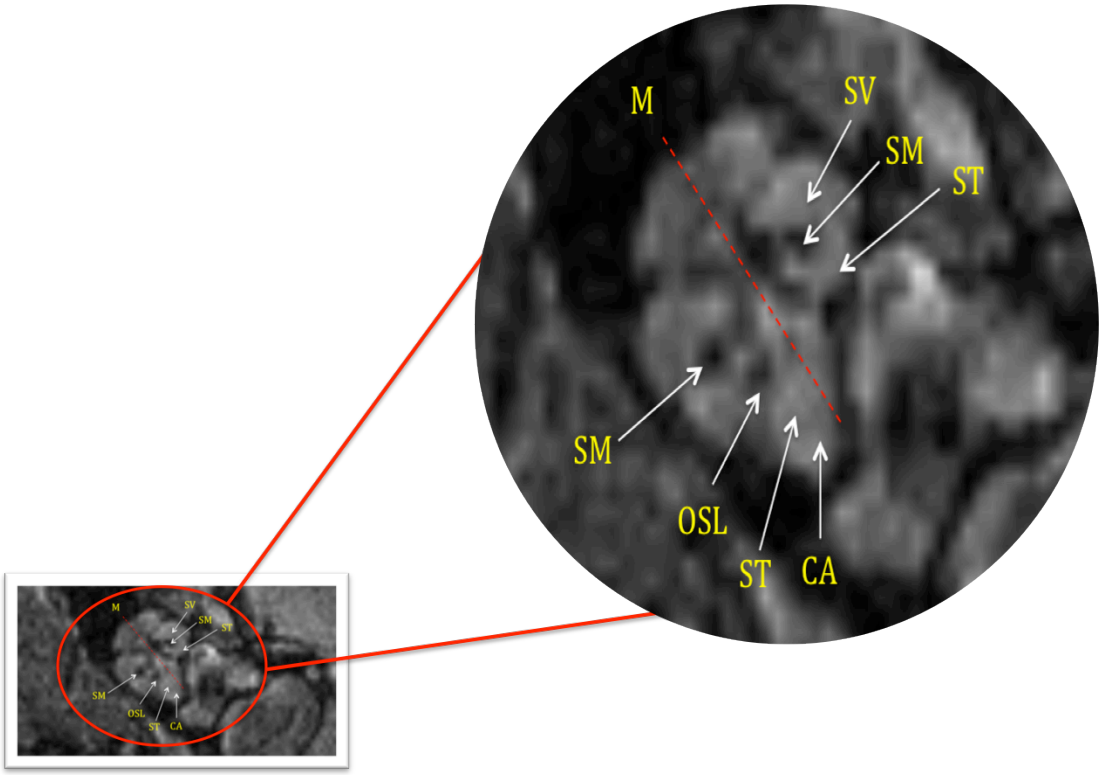

Figure 6.3. Sagittal section through Cochlea. A T1-weighted image; Resolution is 77×77×77 µm3. The structure adjacent to ST is suspected to be CA with signal intensity similar to ST. Abbreviations: CA: Cochlear aqueduct, Mod: Modiolus, OSL: Osseous Spiral Lamina, SM: Scala Media, ST: Scala Tympani, SV: Scala Vestibuli.

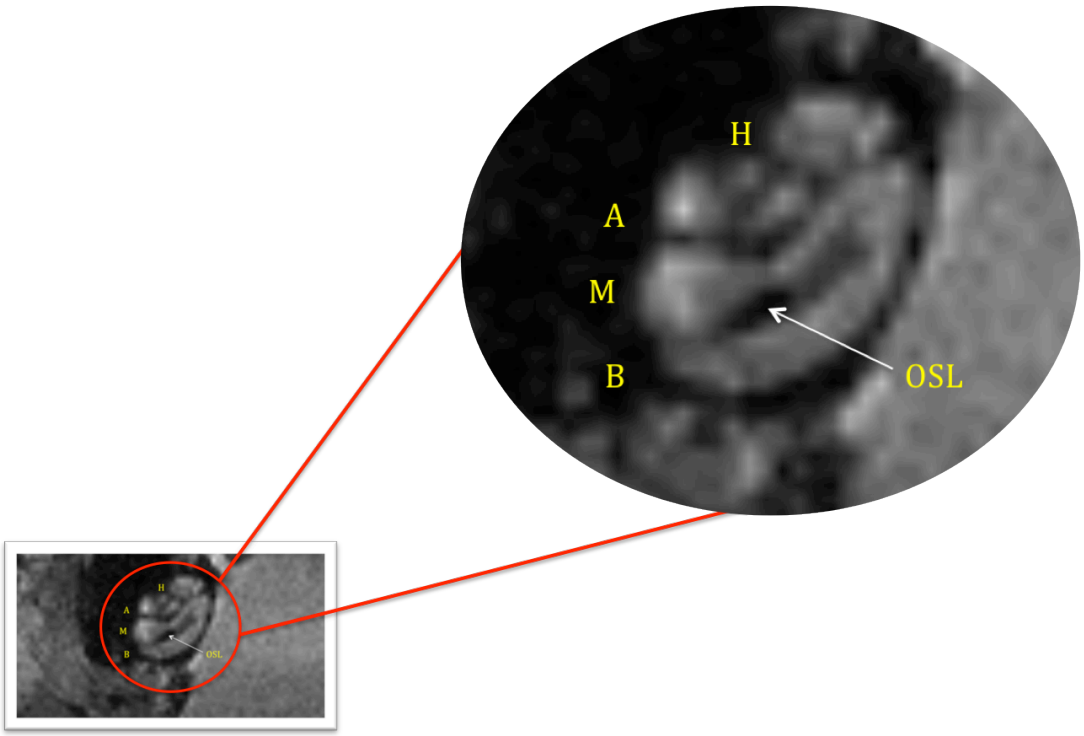

Figure 6.4. Axial Section through the cochlea. A T1-weighted image; Resolution is 77×77×77 µm3. Abbreviations: A: Apical Turn, M: Middle Turn, B: Basal Turn, H: Helicotrema, OSL: Osseous Spiral Lamina